JOURNAL OF AIRCRAFT
Vol. 29, No. 6, Nov.–Dec. 1992

Longitudinal Stability Analysis of Aerial-Towed Systems

Noriaki Nakagawa* and Akira Obata†
Japan Aircraft Manufacturing Company, Ltd., Yokohama 236, Japan

This paper presents an investigation into the longitudinal stability of aerial-towed systems consisting of a flexible, inextensible cable having a circular cross section and a symmetric rigid towed body. Coupled small motions of the towed system about steady-state conditions are studied. Equations governing the towed system are derived by the application of Lagrange's equations under an approximation in which the cable motion is expressed by finite degrees of freedom. Various modes and their stability are obtained by solving the eigenvalue problem of the linearized equations of motion. Three typical unstable motions are introduced by parametric studies of three types of towed systems and their stability conditions are examined.

Introduction

TOWED systems, such as towed aerial vehicles and submersibles, are widely used in scientific research and military fields. In general, these towed systems are required to have not only static stability but also dynamic stability. Glauert[1] developed a simplified method using "cable derivatives," and investigated the dynamic stability of the towed system. This method has been recognized as a convenient tool for its simplicity. However, cable motions are not considered rigorously in the method, so that later, many researchers tried to examine towed system dynamics more exact. Choo and Casarella[2] reviewed these studies and grouped them from the viewpoint of the cable dynamic treatment, as follows: 1) equivalent lumped-mass method; 2) linearization method; 3) method of characteristics; 4) finite element method; and 5) other methods.

In the first method, the study is focused mainly on the towed-body motion, and governing equations having added terms representing the cable effects are derived. This method incorporates Glauert's method of "cable derivatives" and was extensively applied by Jeffrey[3] to investigate the stability of an underwater towed body.

In the second method, the exact governing equations containing the cable behavior are linearized under the assumption of small perturbations from the equilibrium state. Using this method, DeLaurier[4] and Abel[5] examined towed systems with cables having shallow and zero curvature, respectively. However, the general stability problem including the motion of a cable with large curvature has still not been adequately treated.

The third method, developed by Huffman and Genin,[6] Cannon and Genin,[7] is used to solve the exact governing equations numerically.

In the fourth method the cable equations of motion are formulated under an approximation where the cable is replaced by a finite number of elements and are expressed as simultaneous ordinary differential equations. The simulated behavior of towed systems under various initial and boundary conditions are discussed in Refs. 8–16. However, the third and fourth methods are generally not appropriate for stability problems because excessive computing time or numerous finite elements are needed to obtain sufficient accuracy.

This article presents a different approach to the application of the linearization method for examining the stability problem of general towed systems. For simplicity, the cable is assumed to be flexible and inextensible. The cable motions are approximated by a series of admissible functions and expressed by a finite number of generalized coordinates. The governing equations in terms of the generalized coordinates are derived by applying Lagrange's equations of motion. The resulting simultaneous ordinary differential equations are then linearized, and the stability is examined by solving the eigenvalue problem of the linear system.

To facilitate understanding of the factors contributing to the stability of the towed system, two simplified systems will be examined before the general problem is analyzed. The first system, that is the simplest case, has a sphere as the towed body and a cable with a straight configuration in the steady state. Drag is the only aerodynamic force considered to act on the sphere. The effects of the sphere size on the system stability are examined, and unstable oscillations of the cable towing a small sphere are obtained. The second system has an ordinary towed-body shape. However, the cable configuration is assumed to be the same as that of the first system. In this case, the aerodynamic effects of the towed body on the stability are investigated, and an unstable pitching motion of the towed body is presented. The final investigation is of a general system consisting of a cable in a curved configuration at steady state and a towed body. Almost all of a typical towed system's features are included in this model. Effects of the aerodynamic characteristics of the towed body on the stability are studied by a parametric study, and an unstable "bowing" motion of the system[1] is introduced.

Governing Equations

Towed System Model

The aerial-towed system considered in this article consists of a long cable and a symmetrical rigid towed body, as shown in Fig. 1. The towing aircraft is assumed to maintain a steady level flight with constant speed U_0. The cable is assumed to be completely flexible and inextensible and to have a circular cross section. Since the cable is assumed to be inextensible, total length denoted by L is constant, and an arbitrary point on the cable is expressed by the length s.

The two-dimensional problem of the coupled motions of the cable-body system are treated, and three rectangular coordinate systems will be used to develop the equations of motion. These are:

1) The aircraft-fixed coordinate system (X_P, Z_P) with the origin at the connecting point of the cable, the X_P-axis lying parallel to the constant speed direction U_O, and the Z_P-axis in the direction of gravity. The unit vectors in the directions of the X_P- and Z_P-axes are denoted by i_1 and i_3, respectively.

2) The cable-fixed coordinate system (X_C, Z_C) with the origin at an arbitrary point s of the cable, and the X_C-axis tangential to the cable at this point. The unit vectors in the

Received May 14, 1990; revision received Oct. 15, 1991; accepted for publication Oct. 29, 1991.

*Assistant Manager, Engineering Division. Member AIAA.
†Senior Manager, Engineering Division. Member AIAA.

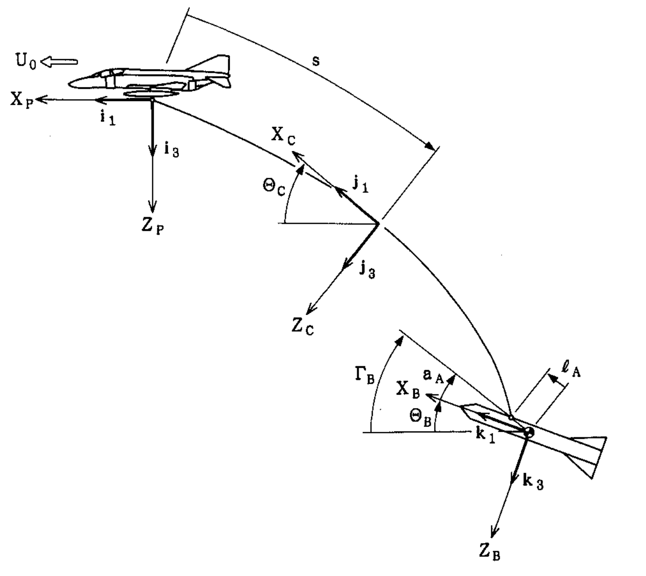

Fig. 1 Aerial towed system.

directions of the X_C- and Z_C-axes are denoted by j_1 and j_3, respectively.

3) The body-fixed coordinate system (X_B, Z_B) with the origin at the center of gravity of the towed body, the X_B-axis in the forward direction and the Z_B-axis in the downward direction, in the symmetrical plane. The unit vectors in the directions of the X_B- and Z_B-axes are denoted by k_1 and k_3, respectively.

The aircraft fixed-coordinate system (X_P, Z_P) is also considered to be an inertial system because of the assumed steady-flight condition of the aircraft. The geometrical relations of the unit vectors defined in each coordinate system are as follows:

$$\begin{bmatrix} j_1 \\ j_3 \end{bmatrix} = \begin{bmatrix} \cos\Theta_C & -\sin\Theta_C \\ \sin\Theta_C & \cos\Theta_C \end{bmatrix} \cdot \begin{bmatrix} i_1 \\ i_3 \end{bmatrix} \tag{1}$$

$$\begin{bmatrix} k_1 \\ k_3 \end{bmatrix} = \begin{bmatrix} \cos\Theta_B & -\sin\Theta_B \\ \sin\Theta_B & \cos\Theta_B \end{bmatrix} \cdot \begin{bmatrix} i_1 \\ i_3 \end{bmatrix} \tag{2}$$

where, $\Theta_C(t, s)$ and $\Theta_B(t)$ are the pitch angles of the cable at s and the towed body, respectively. $\Theta_B(t)$ is also represented by the equation

$$\Theta_B(t) = \Gamma_B(t) - a_A \tag{3}$$

where, $\Gamma_B(t)$ and a_A are the angles of the segment ℓ_A between X_P-axis and X_B-axis, respectively, as shown in Fig. 1.

In view of the assumption of cable inextensibility, the position vector of an arbitrary point of the cable r_C and the towed body r_B with respect to the aircraft fixed coordinate system (X_P, Z_P) is expressed as follows:

$$r_C(t, s) = \left[-\int_0^s \cos\Theta_C \, ds \right] i_1 + \left[\int_0^s \sin\Theta_C \, ds \right] i_3 \tag{4}$$

$$r_B(t, x_B, z_B) = r_C(t, L) + [-\ell_A \cos\Gamma_B] i_1 + [\ell_A \sin\Gamma_B] i_3 + x_B k_1 + z_B k_3 \tag{5}$$

Equations (2–5) allow the position vector of any point in the system to be described by two angles, $\Theta_C(t, s)$ and $\Gamma_B(t)$.

The towed system is considered to move around a steady-state configuration, so that the motion of the system can be separated into steady-state and perturbed motions. The cable perturbed motion is further approximated in a form with N finite degrees of freedom. Then, $\Theta_C(t, s)$ and $\Gamma_B(t)$ are given by

$$\Theta_C(t, s) = \Theta_{Co}(s) + \sum_{n=1}^{N} k_n(t)\phi_n(s) \tag{6}$$

$$\Gamma_B(t) = \Gamma_{Bo} + \gamma_B(t) \tag{7}$$

where, subscript "o" denotes steady state.

In light of the assumption of cable flexibility, no geometrical boundary conditions of the cable, such as the cable angle Θ_C or the cable's curvature at either end, are imposed by any connecting conditions. In this article, mutually orthogonal functions introduced in Appendix A are employed as mode functions $\phi_n(s)$, as follows:

$$\phi_n(s) = \sin\left[\frac{n\pi s}{L}\right] \qquad (n = 1, 2, \ldots, N-1) \tag{8}$$

$$\phi_n(s) = \frac{s}{L} - \sum_{m=1}^{N-1} (-1)^{m-1} \frac{2}{m\pi} \sin\left[\frac{m\pi s}{L}\right] \qquad (n = N) \tag{9}$$

Since the functions $\phi_n(s)$ ($n = 1, 2, \ldots, N-1$) provided by Eq. (8) vanish at both ends, $s = 0$ and $s = L$, the function $\phi_N(s)$ supplied by Eq. (9) is introduced to satisfy the arbitrary cable-angle condition at $s = L$. The arbitrary cable-angle condition at $s = 0$ is not satisfied by using the above mode functions. However, the influence of the error is considered to be insignificant, because no internal moment exists in the cable due to the assumption of flexibility.

Substituting Eq. (7) into Eq. (3), the pitch angle of the towed body $\Theta_B(t)$ is given as

$$\Theta_B(t) = \Theta_{Bo} + \gamma_B(t) \tag{10}$$

where

$$\Theta_{Bo} = \Gamma_{Bo} - a_A \tag{11}$$

Therefore, the motions of the towed system are described by the finite functions $k_n(t)$ ($n = 1, 2, \ldots, N$) and $\gamma_B(t)$.

Equations of Motion

The equations of motion of the towed system are derived by applying Lagrange's equation of motion. In view of the assumptions that the towed body is rigid and the cable is flexible and inextensible, no strain energy exists in the towed system. Therefore, according to Washizu,[17] the equations of motion are expressed as

$$\frac{d}{dt}\left(\frac{\partial T}{\partial \dot{q}_i}\right) - \frac{\partial T}{\partial q_i} = Q_i \qquad (i = 1, 2, \ldots, N+1) \tag{12}$$

where, q_i are generalized coordinates

$$q_1 = k_1(t),\ q_2 = k_2(t),\ \ldots,\ q_N = k_N(t),\ q_{N+1} = \gamma_B(t) \tag{13}$$

and, the total kinetic energy of the towed system T and the generalized forces acting on the towed system Q_i ($i = 1, 2, \ldots, N+1$) are defined as

$$T = \frac{1}{2}\int_0^L \mu_C \left(\frac{dr_C}{dt}\right)^2 ds + \frac{1}{2}\iiint_{V(B)} \rho_B \left(\frac{dr_B}{dt}\right)^2 dV_B \tag{14}$$

$$Q_i = \int_0^L (\mu_C g i_3)\cdot\left(\frac{\partial r_C}{\partial q_i}\right) ds + \int_0^L F_C \cdot \left(\frac{\partial r_C}{\partial q_i}\right) ds + \iiint_{V(B)} (\rho_B g i_3)\cdot\left(\frac{\partial r_B}{\partial q_i}\right) dV_B + \iint_{S(B)} F_B \cdot \left(\frac{\partial r_B}{\partial q_i}\right) dS_B \qquad (i = 1, 2, \ldots, N+1) \tag{15}$$

where, μ_C, ρ_B, g, F_C and F_B are the mass per unit length of the cable, the density of the towed body, the gravitational acceleration, the aerodynamic force acting on the unit length of the cable, and the aerodynamic force acting on the unit area on the towed body surface, respectively.

The aerodynamic force acting on a cable has been studied by many researchers as summarized by Casarella and Parsons.[18] In the present paper, $\boldsymbol{F}_C$ is expressed according to Hoerner[19] under the assumption of the crossflow-principle at subcritical Reynold's number, as

$$\boldsymbol{F}_C(t, s) = A_x\boldsymbol{j}_1 + A_z\boldsymbol{j}_3 \tag{16}$$

and

$$A_x(t, s) = -\tfrac{1}{2}\rho d U_C[\pi c_f(U_C^2 + W_C^2)^{1/2}] \tag{17}$$

$$A_z(t, s) = -\tfrac{1}{2}\rho d W_C[\pi c_f(U_C^2 + W_C^2)^{1/2} + c_p|W_C|] \tag{18}$$

where, ρ, d, π, c_f and c_p denote the density of the air, the diameter of the cable, the circular constant, the friction drag coefficient, and pressure drag coefficient of the cable, respectively. U_C and W_C are the velocity components, and are derived from Eqs. (4), (6), and (1) as

$$U_O\boldsymbol{i}_1 + \frac{\mathrm{d}\boldsymbol{r}_C}{\mathrm{d}t} = (U_O + U_S)\boldsymbol{i}_1 + W_S\boldsymbol{i}_3 = U_C\boldsymbol{j}_1 + W_C\boldsymbol{j}_3 \tag{19}$$

where

$$U_S(t, s) = \int_0^s \left(\sum_{n=1}^N \dot{k}_n\phi_n\right) \sin\Theta_C \,\mathrm{d}s \tag{20}$$

$$W_S(t, s) = \int_0^s \left(\sum_{n=1}^N \dot{k}_n\phi_n\right) \cos\Theta_C \,\mathrm{d}s \tag{21}$$

$$U_C(t, s) = (U_O + U_S)\cos\Theta_C - W_S\sin\Theta_C \tag{22}$$

$$W_C(t, s) = (U_O + U_S)\sin\Theta_C + W_S\cos\Theta_C \tag{23}$$

The total aerodynamic force and moment acting on the towed body, expressed with respect to the body fixed coordinates (X_B, Z_B), are now considered. The force and moment are obtained by the integration of the local force $\boldsymbol{F}_B$ and its moment, and are defined as

$$\iint_{S(B)} \boldsymbol{F}_B \,\mathrm{d}S_B = X_a\boldsymbol{k}_1 + Z_a\boldsymbol{k}_3 \tag{24}$$

$$\iint_{S(B)} (x_B\boldsymbol{k}_1 + z_B\boldsymbol{k}_3) \times \boldsymbol{F}_B \,\mathrm{d}S_B = M_a\boldsymbol{k}_2 \tag{25}$$

where

$$\boldsymbol{k}_2 = \boldsymbol{k}_3 \times \boldsymbol{k}_1 \tag{26}$$

In general, the aerodynamic forces X_a, Z_a, and moment M_a are considered functions of the velocity components U_B, W_B, and the pitching angular velocity q_B of the towed body. U_B and W_B are given from Eqs. (5), (7), (20), (21), and (2) as

$$\begin{aligned} U_O\boldsymbol{i}_1 + \left.\frac{\mathrm{d}\boldsymbol{r}_B}{\mathrm{d}t}\right|_{X_B=Z_B=0} &= (U_O + U_s(t, L) + \dot{\gamma}_B\cdot\ell_A\sin\Gamma_B)\boldsymbol{i}_1 \\ &\quad + (W_s(t, L) + \dot{\gamma}_B\cdot\ell_A\cos\Gamma_B)\boldsymbol{i}_3 \\ &= U_B\boldsymbol{k}_1 + W_B\boldsymbol{k}_3 \end{aligned} \tag{27}$$

where

$$\begin{aligned} U_B(t) &= (U_O + U_S(t, L) + \dot{\gamma}_B\cdot\ell_A\sin\Gamma_B)\cos\Theta_B \\ &\quad - (W_S(t, L) + \dot{\gamma}_B\cdot\ell_A\cos\Gamma_B)\sin\Theta_B \end{aligned} \tag{28}$$

$$\begin{aligned} W_B(t) &= (U_O + U_S(t, L) + \dot{\gamma}_B\cdot\ell_A\sin\Gamma_B)\sin\Theta_B \\ &\quad + (W_S(t, L) + \dot{\gamma}_B\cdot\ell_A\cos\Gamma_B)\cos\Theta_B \end{aligned} \tag{29}$$

The pitching angular velocity $q_B(t)$ is obtained from Eq. (10) as

$$q_B(t) = \frac{\mathrm{d}\Theta_B}{\mathrm{d}t} = \dot{\gamma}_B \tag{30}$$

Therefore, the total kinetic energy T and the generalized force Q_i are obtained by substituting Eqs. (1–11) and (16–26) into Eqs. (14) and (15). Consequently, the equations of motion derived by Lagrange's Eq. (12) are expressed as

$$a_n\ddot{\gamma}_B + b_n\dot{\gamma}_B^2 + \sum_{i=1}^N c_{n,i}\ddot{k}_i + \sum_{i=1}^N\sum_{j=1}^N d_{n,ij}\dot{k}_i\dot{k}_j + e_n = 0 \qquad (n = 1, 2, \ldots, N) \tag{31}$$

$$a_{N+1}\ddot{\gamma}_B + \dot{\gamma}_B\sum_{i=1}^N b_{N+1,i}\dot{k}_i + \sum_{i=1}^N c_{N+1,i}\ddot{k}_i + \sum_{i=1}^N\sum_{j=1}^N d_{N+1,ij}\dot{k}_i\dot{k}_j + e_{N+1} = 0 \tag{32}$$

where the coefficients are

$$a_n = m_B\ell_A\int_0^L \phi_n\cos(\Gamma_B - \Theta_C)\,\mathrm{d}s \tag{33}$$

$$b_n = -m_B\ell_A\int_0^L \phi_n\sin(\Gamma_B - \Theta_C)\,\mathrm{d}s \tag{34}$$

$$c_{n,i} = m_B(X_{Gi}X_{Gn} + Z_{Gi}Z_{Gn}) + \int_0^L \mu_C(X_{Ci}X_{Cn} + Z_{Ci}Z_{Cn})\,\mathrm{d}s \tag{35}$$

$$\begin{aligned} d_{n,ij} &= m_B\left(X_{Gn}\int_0^L \phi_i\phi_j\cos\Theta_C\,\mathrm{d}s - Z_{Gn}\cdot\int_0^L \phi_i\phi_j\sin\Theta_C\,\mathrm{d}s\right) + \int_0^L \mu_C\left(X_{Cn}\int_0^s \phi_i\phi_j\cos\Theta_C\,\mathrm{d}s\right. \\ &\quad \left. - Z_{Cn}\int_0^s \phi_i\phi_j\sin\Theta_C\,\mathrm{d}s\right)\mathrm{d}s \end{aligned} \tag{36}$$

$$\begin{aligned} e_n &= -(X_a\cos\Theta_B + Z_a\sin\Theta_B)X_{Gn} \\ &\quad - (-X_a\sin\Theta_B + Z_a\cos\Theta_B + m_B g)Z_{Gn} \\ &\quad - \int_0^L [(A_x\cos\Theta_C + A_z\sin\Theta_C)X_{Cn} \\ &\quad + (-A_x\sin\Theta_C + A_z\cos\Theta_C + \mu_C g)Z_{Cn}]\,\mathrm{d}s \end{aligned} \tag{37}$$

$$a_{N+1} = I_y + m_B\cdot\ell_A^2 \tag{38}$$

$$b_{N+1,i} = -m_B\ell_A\int_0^L \phi_i\sin(\Gamma_B - \Theta_C)\,\mathrm{d}s \tag{39}$$

$$c_{N+1,i} = m_B\ell_A \int_0^L \phi_i \cos(\Gamma_B - \Theta_C)\, ds \tag{40}$$

$$d_{N+1,ij} = m_B\ell_A \int_0^L \phi_i\phi_j \sin(\Gamma_B - \Theta_C)\, ds \tag{41}$$

$$e_{N+1} = -(m_B g\cdot\ell_A \cos\Gamma_B + X_a\cdot\ell_A \sin a_A + Z_a\cdot\ell_A \cos a_A + M_a) \tag{42}$$

$$m_B = \iiint_{V(B)} \rho_B\, dV_B \tag{43}$$

$$I_y = \iiint_{V(B)} (z_B^2 + x_B^2)\rho_B\, dV_B \tag{44}$$

$$X_{Cn}(t, s) = \int_0^s \phi_n\cdot\sin\Theta_C\, ds, \qquad Z_{Cn}(t, s) = \int_0^s \phi_n\cdot\cos\Theta_C\, ds \qquad (n = 1, 2, \ldots, N) \tag{45}$$

$$X_{Gn}(t) = X_{Cn}(t, L), \qquad Z_{Gn}(t) = Z_{Cn}(t, L) \qquad (n = 1, 2, \ldots, N) \tag{46}$$

Linearized Equations

Linearized equations of motion of a towed system are derived under the assumption that the perturbations of motion are small. These perturbations are expressed by using the generalized coordinates q_i ($i = 1, 2, \ldots, N + 1$) defined by Eq. (13) as previously mentioned. Considering the fact that the generalized coordinates are nondimensional values describing angle, the linearized equations are derived by setting

$$\gamma_B(t) << 1, \qquad k_n(t) << 1 \qquad (n = 1, 2, \ldots, N) \tag{47}$$

in Eqs. (31) and (32), and neglecting the second order products of the generalized coordinates. Then

$$a'_n\ddot{\gamma}_B + \sum_{i=1}^{N} c'_{n,i}\ddot{k}_i + e'_n = 0 \qquad (n = 1, 2, \ldots, N) \tag{48}$$

$$a_{N+1}\ddot{\gamma}_B + \sum_{i=1}^{N} c'_{N+1,i}\ddot{k}_i + e'_{N+1} = 0 \tag{49}$$

where, the coefficients a'_n, $c'_{n,i}$, and $c'_{N+1,i}$ are derived from Eqs. (33), (35), and (40) under the steady state condition; and e'_n, e'_{N+1} are obtained from Eqs. (37) and (42) by the linearization with respect to the generalized coordinates.

In this approximation, the aerodynamic force and moment, X_a, Z_a, M_a, acting on the towed body are separated into steady and perturbational values, and linearized in a manner similar to that used in the analysis of ordinary airplane dynamics, as follows:

$$X_a(t) = X_{a0} + m_B(X_u\cdot u_B + X_w\cdot w_B) \tag{50}$$

$$Z_a(t) = Z_{a0} + m_B(Z_u\cdot u_B + Z_w\cdot w_B + Z_{\dot{w}}\cdot \dot{w}_B + Z_q\cdot q_B) \tag{51}$$

$$M_a(t) = M_{a0} + I_y(M_u\cdot u_B + M_w\cdot w_B + M_{\dot{w}}\cdot\dot{w}_B + M_q\cdot q_B) \tag{52}$$

where, dimensional stability derivatives $X_u, X_w, \ldots, M_q$ of the towed body are determined about the steady-state condition. Small perturbation motions u_B and w_B are provided from velocity components U_B and W_B defined by Eqs. (28) and (29) by the linearization with respect to the generalized coordinates. The pitching angular velocity q_B is given by Eq. (30).

Therefore, Eqs. (48) and (49) are further rewritten as an $N + 1$ order linear system

$$M\ddot{x} + C\dot{x} + Kx = 0 \tag{53}$$

where, M, C, K are coefficient matrices, and x is a vector of generalized coordinates:

$$x = (\gamma_B, k_1, k_2, \ldots, k_N)^T \tag{54}$$

Stability Analysis

Case 1. Towed Sphere System

Towed systems consisting of a spherical towed body and a cable with a straight configuration at the steady state are treated in this case. Various diameters of the towed sphere are considered, and the size effects on the dynamic characteristics of the system are examined. The data of the system model are given in Table 1. The cable is assumed to have a constant diameter along its length. The diameter and mass per unit length are of the same order as a stranded steel wire used in typical towed systems. The sphere is assumed to be made of homogeneous material, and the drag is considered to be the only aerodynamic force acting on the sphere. The mass of the sphere is determined for each sphere size to produce the straight cable configuration with "critical angle."[20]

The stability of this model is analyzed under the condition of 30 functions ϕ_n defined by Eqs. (8) and (9). The eigenvalues of Eq. (53) are solved numerically. The stability and frequency of the motion of this model are evaluated from the real and imaginary parts of the eigenvalue, respectively. The mode shape of the motion is obtained from the relative eigenvector.

The stability of a large towed sphere, 100 cm in diameter, is analyzed, and the results are shown in Fig. 2. This towed sphere system is stable, and the eigenvalues are grouped into three mode types called "pendulum mode," "pitching mode," and various order "vibration mode." The pendulum mode expresses a simple pendulum motion of the sphere. The pitching mode shows a large pitching motion of the sphere with weak damping. The vibration modes indicate vibrations of the cable, and appear similar to vibrations of a string with fixed ends. This similarity is considered to be caused by the large cable tension due to the large sphere drag force.

Since the perturbation of the cable angle expressed by Eq. (6) is approximated to vanish at $s = 0$, the cable angles of the mode shapes shown in Fig. 2 tend to the critical angle at the end connected to the aircraft. Then, the mode shapes have a large curvature near the end, however, the curvature is limited to the extremely small region as shown in Fig. 2. This phenomenon is allowed by the assumption of complete flexibility of the cable. Therefore, the influence of the approximation of the cable angle is insignificant.

The stability of the towed system for several sizes of small spheres are examined. As the sphere size decreases, the eigenvalues of the vibration mode split symmetrically into two

Table 1 Data of towed sphere system

Cable data		
Length	L	100 m
Diameter	d	2.5 mm
Mass per unit length	μ_C	30 g/m
Drag coefficient	c_f	0.02
	c_p	1.2
Sphere data		
Diameter	D	1–100 cm
Drag coefficient	C_D	0.47 (based on front area)
Flight condition		
Speed	U_O	100 m/s
Air density	ρ	1.225 kg/m³

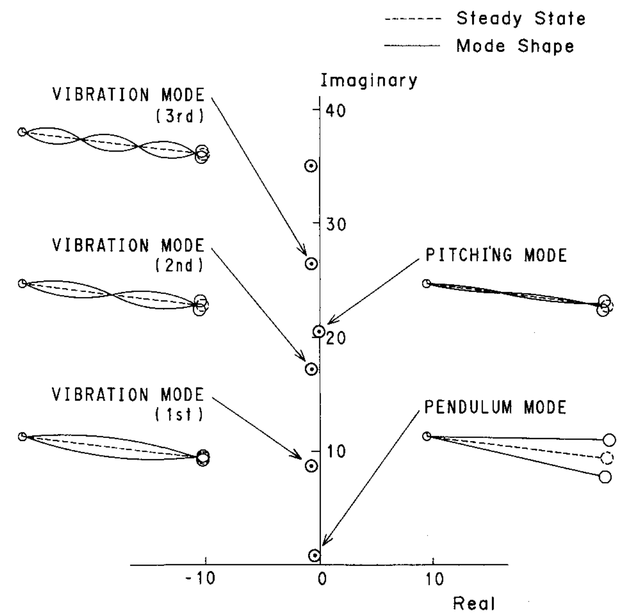

Fig. 2 Stability of a large towed sphere system (diameter = 100 cm).

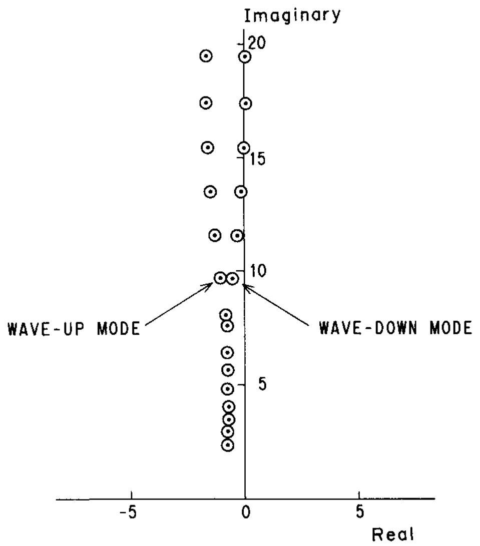

Fig. 3 Stability of a small towed sphere system (diameter = 8 cm).

new vibration modes as shown in Fig. 3 for 8 cm diam and Fig. 4 for 1 cm diam. These new modes express wave motions of the cable, called "wave-down" and "wave-up" modes, with reference to the direction of wave travel. The frequencies that the new vibration modes first appear decreases as the sphere size decreases. As shown in Fig. 4, for the smallest diameter sphere, almost all of the vibration modes are split into the new modes, and some of the wave-down modes become unstable. In view of the small effects of the sphere on the cable motion, the unstable motion is considered to be caused by the cable's own dynamic characteristics under a small tension. These two modes appearing in the small region near the tip of the cable are very similar, however, the directions of the wave motions are opposite each other. In the wave-down mode, the waves proceed down the cable in the direction of the airflow.

In summary, the towed sphere system tends to be unstable when the sphere is small. The unstable motion of the wave-down mode is also similar to "flag flutter" and is called "cable flutter" in this article.

Case 2. Towed System with a Straight Cable Configuration

The aerodynamic effects of a towed body on the system dynamics are examined in this case. The model considered

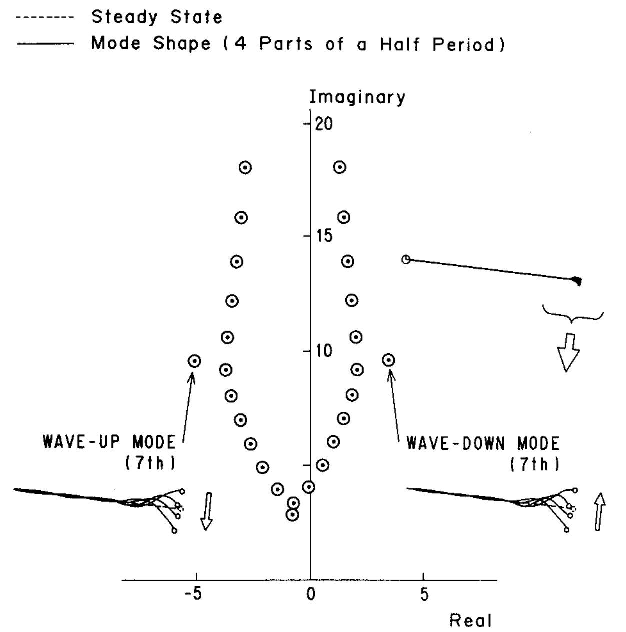

Fig. 4 Stability of a small towed sphere system (diameter = 1 cm).

Table 2 Data of towed body

Diameter of fuselage		0.18 m
Length of fuselage		2.5 m
Mass	m_B	25 kg
Moment of inertia	I_y	11 kg·m^2
Drag coefficient	C_D	0.4 (based on front area)
Stability derivatives	X_u	−0.0510
	X_w	(neglected)
	Z_u	0.0127
	Z_w	−0.841
	$Z_{\dot{w}}$	(neglected)
	Z_q	−0.358
	M_u	0.0123
	M_w	−0.814
	$M_{\dot{w}}$	(neglected)
	M_q	−0.348

here is equivalent to the towed sphere model of case 1 except that the towed body consists of a slender fuselage, wings, and tail fins. The data relating to the towed body and its estimated aerodynamic characteristics are given in Table 2. The incidence angle of the wings is suitably adjusted to produce the straight cable configuration with critical angle at steady state.

The stability of the model is analyzed by solving the eigenvalue problem in the same way as in case 1. From the results shown in Fig. 5, it is apparent that this towed system is stable. The eigenvalues are grouped into three mode types in a manner similar to the towed sphere system, and are again called "pendulum mode," "pitching mode," and "vibration mode." The pendulum mode is an oscillation with the towed body exhibiting a "heaving" motion similar to that of case 1. In the pitching mode, the towed body executes a pitching motion accompanied with a small cable motion. This mode is similar to a short period mode of an ordinary airplane because of the similarity of the aerodynamic characteristics. The vibration modes express various orders of vibration of the cable and relatively small motions of the towed body.

A parametric study is conducted by changing the stability derivatives of the towed body from those of the basic model. This study is limited to the domain that the towed body maintains static pitch stability ($M_w < 0$). The significant results are shown in Fig. 6. The frequency and damping of the pitching mode are dominantly affected by M_w and Z_w (<0), respectively. The effects of the other derivatives on the pitching mode are small and negligible. The pitching mode of a towed body having a large absolute value of Z_w and a small absolute

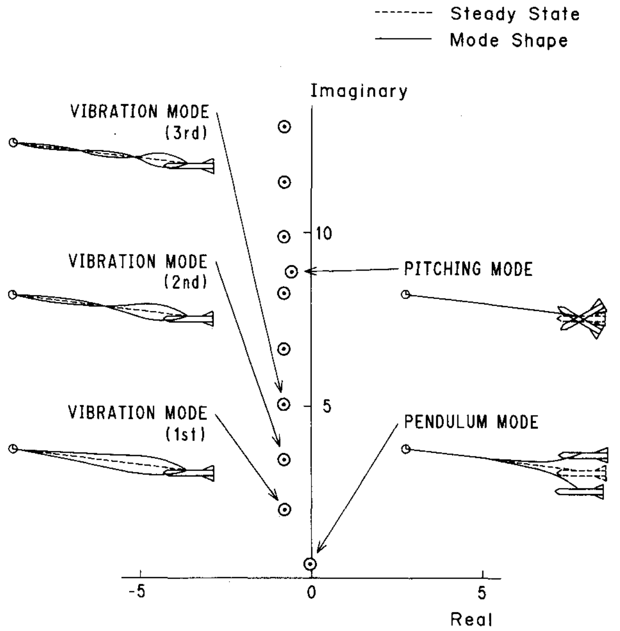

Fig. 5 Stability of a towed system with a straight cable configuration.

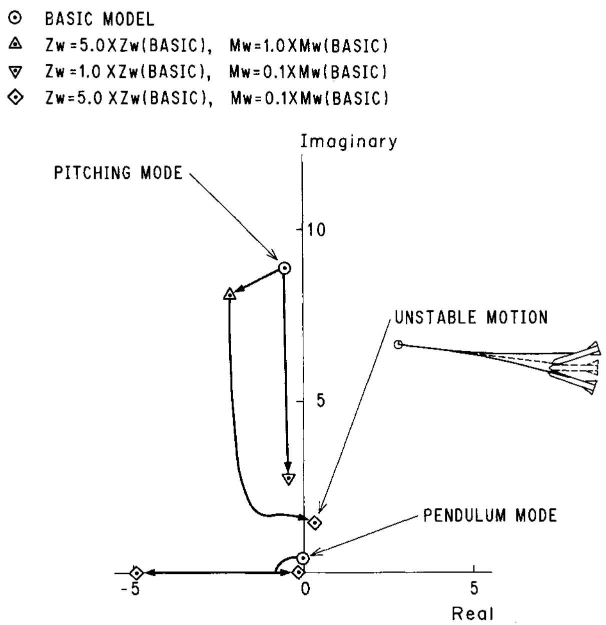

Fig. 6 Parametric study (1)—aerodynamic characteristics.

value of M_w becomes unstable as shown in Fig. 6. In this unstable mode, the towed body not only has a pitching motion but also a heaving motion similar to the pendulum mode.

The pendulum mode is also affected by the stability derivatives Z_w and M_w. This mode changes into two overdamped motions when the absolute value of M_w becomes small in the example with a large absolute value of Z_w. The pendulum mode remains in the stable region throughout this study, and the effects of the other stability derivatives on this mode are negligible.

The vibration modes are almost wholly unaffected by the aerodynamic characteristics of the towed body. This result is considered to be caused by the small disturbance of the aerodynamic force acting on the towed body due to the small perturbation motion of the towed body in these modes.

The conclusions that can be drawn from the parametric study in this case are as follows. The most significant aerodynamic characteristics of the towed body for the system stability are the stability derivatives Z_w and M_w. These derivatives strongly affect the pitching mode and the pendulum mode. An unstable motion of the pitching mode occurs in the case of a large absolute value of Z_w and a small absolute value of M_w. This unstable motion of the pitching mode is called "pitching flutter" in this paper.

Case 3. Towed System with a Curved Cable Configuration

The stability problem of a towed system with a curved cable and a towed body is considered in this case. This model is obtained from the basic model of case 2 by setting the incidence angle of the towed body wings to zero. Other conditions are assumed to be equivalent to the basic model of case 2. In this model, the cable configuration at the steady state is bent due to the weight of the towed body, and the cable tension is larger than the model of case 2.

The stability problem of the basic model is solved in the same manner as in the previous cases and the results are shown in Fig. 7. The eigenvalues of this model are stable and are grouped into four modes called "pendulum mode," "pitching mode," "vibration mode," and new "bowing mode." The bowing mode is characterized by having a cable "bowing" oscillation with the towed body "surging" fore and aft. This mode corresponds to the first-order vibration mode of the towed system with straight cable configuration mentioned in case 2 but is changed due to the cable curvature. In this mode, the motion of a towed body with large mass produces slower frequency and smaller damping of motion than those of the first order vibration mode. The other modes are essentially identical to those of the towed system in case 2 except that the vibration modes have a higher frequency and a stronger damping. These phenomena are caused by the larger cable tension and the larger aerodynamic force acting on the cable due to the large inclination near the towed body, respectively.

A parametric study similar to that of case 2 gives the following results: The stability of the bowing mode is strongly affected by the stability derivatives $Z_w(<0)$ and $M_w(<0)$ of the towed body, as shown in Fig. 8. When the absolute value of Z_w becomes large or the absolute value of M_w becomes small, the bowing mode becomes unstable. A distinguishing feature of the unstable bowing mode is the direction of motion of the towed body. When the bowing mode is stable as shown in Fig. 7, the towed body describes an ellipsoid in the counterclockwise direction around the steady position. However, the orbital motion of the towed body in the unstable bowing mode draws an ellipsoid in the opposite direction as shown in Fig. 8. These phenomena are discussed in Appendix B. The large drag of the towed body increases the stability, how-

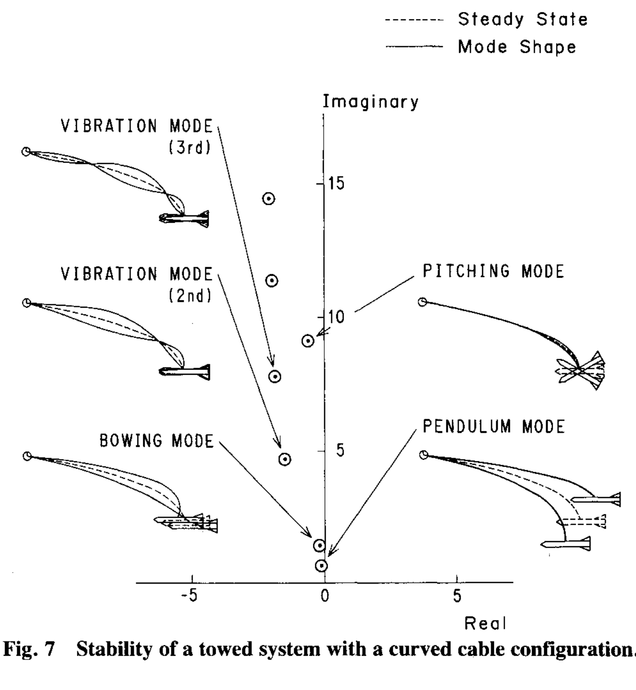

Fig. 7 Stability of a towed system with a curved cable configuration.

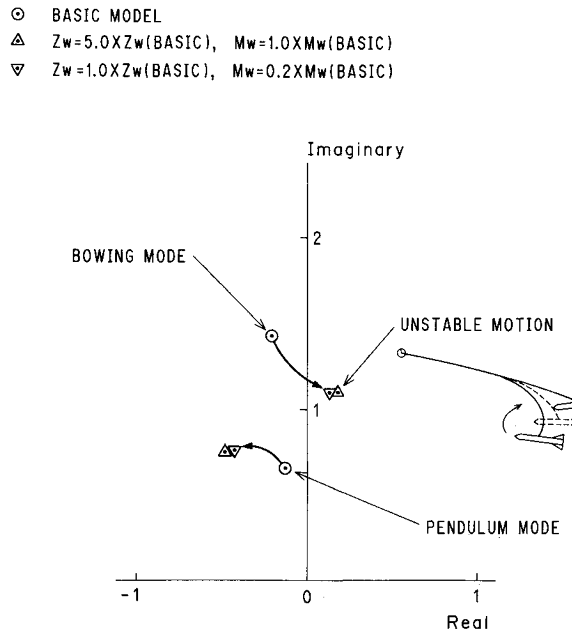

Fig. 8 Parametric study (2)—aerodynamic characteristics.

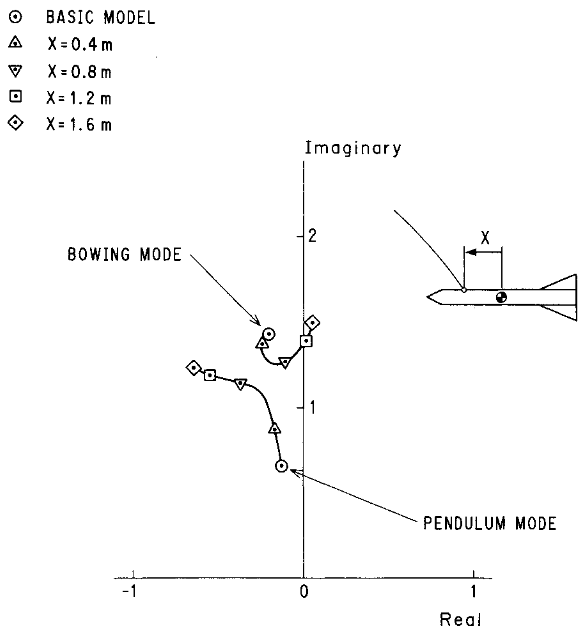

Fig. 9 Parametric study (3)—tow point position.

ever, the effects of the other aerodynamic characteristics on the bowing mode stability are insignificant.

The pendulum mode and the pitching mode are also influenced by the aerodynamic characteristics of the towed body, however, these modes remain within the stable region throughout this analysis. The vibration modes are insignificant for stability of this towed system.

Another parametric study with respect to the tow point position of the towed body is also examined in this case. The stability of the bowing mode and the pendulum mode depend on the position as shown in Fig. 9, and the bowing mode with a tow point locating forward becomes unstable.

The results of the parametric study are briefly stated that the most significant aerodynamic characteristics for the system stability are the stability derivatives Z_w and M_w of the towed body. This conclusion is the same as that for the towed system with straight cable configuration, except for the mode that becomes unstable. The bowing mode given by the cable curvature tends to be unstable when the absolute value of Z_w becomes large or the absolute value of M_w becomes small. The bowing mode also becomes unstable when the tow point is moved forward. The unstable motion of the bowing mode is called "bowing flutter" throughout this paper.

Conclusions

A method of longitudinal stability analysis available for general aerial towed systems has been developed by using the Lagrange's equation of motion. This method is also applied to examine the stability of three cases 1) a towed sphere system with straight cable configuration; 2) a typical towed body system with straight cable configuration; 3) and a typical towed body system with curved cable configuration. Two useful results are obtained from the parametric studies of the models:

1) The behaviour of a towed system around the steady state consists essentially of three types of motion called pendulum mode, pitching mode, and various order vibration modes. However, these modes strongly depend on the conditions of the towed body or the cable. If the towed body becomes small, the vibration modes change into wave-down and wave-up modes. If the towed system has a curved cable configuration at a steady state, the first order vibration mode changes into the bowing mode.

2) The size, the stability derivatives Z_w, M_w, and the tow point position of the towed body are significant for the stability of a towed system. When the size becomes small, unstable motions called cable flutter occur in the wave downmodes. When the absolute values of the stability derivatives Z_w and M_w become large and small, respectively, an unstable motion called pitching flutter or bowing flutter appears. The bowing flutter also appears in the case with the tow point locating forward of the towed body.

Appendix A: Orthogonal Functions

An arbitrary function $f(x)$ in a domain $(0 \leqq x \leqq 1)$ is sometimes approximated by a finite Fourier sine series in engineering fields as

$$f(x) \approx \sum_{n=1}^{N} a_n \sin(n\pi x) \tag{A1}$$

where, a_n are given by

$$a_n = 2 \int_0^1 f(x)\sin(n\pi x)\,dx \qquad (n = 1, 2, \ldots, N) \tag{A2}$$

Considering the orthogonality of the trigonometric functions

$$\begin{aligned} \int_0^1 \sin(n\pi x)\sin(m\pi x)\,dx &= \tfrac{1}{2} \quad \text{for} \quad (m = n) \\ &= 0 \quad \text{for} \quad (m \neq n) \end{aligned} \tag{A3}$$

the residual $R(x)$

$$R(x) = f(x) - \sum_{n=1}^{N} a_n \sin(n\pi x) \tag{A4}$$

is shown to be orthogonal to the finite trigonometric functions, as follows:

$$\begin{aligned} \int_0^1 R(x)\sin(m\pi x)\,dx &= \int_0^1 f(x)\sin(m\pi x)\,dx \\ &- \sum_{n=1}^{N} a_n \int_0^1 \sin(m\pi x)\sin(n\pi x)\,dx \\ &= a_m/2 - a_m/2 \\ &= 0 \qquad (m = 1, 2, \ldots, N) \end{aligned} \tag{A5}$$

When the arbitrary function $f(x)$ are chosen as

$$f(x) = x \tag{A6}$$

the residual function $R(x)$ is expressed as

$$R(x) = x - \sum_{n=1}^{N} (-1)^{n-1} \frac{2}{n\pi} \sin(n\pi x) \tag{A7}$$

and has the boundary values

$$R(0) = 0 \quad \text{and} \quad R(1) = 1 \tag{A8}$$

Appendix B: Stability of the Bowing Mode

The work W done by the cable on the towed body through its ellipsoidal motion can be defined, transformed by Stoke's theorem, and linearized for a small motion as follows:

$$W = \int_C \boldsymbol{T} \cdot \mathrm{d}\boldsymbol{t} = \iint_S \mathrm{rot}\, \boldsymbol{T} \cdot \mathrm{d}\sigma = \omega_y S \tag{B1}$$

$$\boldsymbol{T} = T_x \boldsymbol{i}_1 + T_z \boldsymbol{i}_3, \qquad \omega_y = \frac{\partial T_x}{\partial z_P} - \frac{\partial T_z}{\partial x_P} \tag{B2}$$

where $\boldsymbol{T}$, $\boldsymbol{t}$, and S express the cable tension vector at the tow point, the unit tangential vector on the ellipsoidal motion of the tow point in the clockwise direction, and the area of the ellipsoid, respectively.

The derivatives $\partial T_x / \partial z_P$ and $\partial T_z / \partial x_P$ used in the definition of ω_y are considered as dimensional "cable derivatives." These cable derivatives are determined from steady conditions using small displacements of the tow point, and are derived in this case as

$$\frac{\partial T_x}{\partial z_P} = 2.93 \qquad \frac{\partial T_z}{\partial x_P} = 1.89 \qquad (\mathrm{Kg}_f/\mathrm{m})$$

Then, the value of ω_y defined by Eq. (B2) is positive. Therefore, the work W becomes positive when the tow point moves in the clockwise direction and negative when it moves in the counterclockwise direction, since the integration in Eq. (B1) is defined in the clockwise direction. In other words, positive work increases the kinetic energy of the towed body, and negative work decreases the kinetic energy. Consequently, the stability of the bowing mode depends on the direction of the tow point motion.

Acknowledgment

The authors express their sincere appreciation to A. Azuma of the University of Tokyo for his valuable guidance and advice for a long time.

References

[1]Glauert, H., "The Stability of a Body Towed by a Light Wire," Ames Research Center, R&M No. 1312, 1930, pp. 1331–1352.

[2]Choo, Y., and Casarella, M. J., "A Survey of Analytical Methods for Dynamic Simulation of Cable-Body System," *Journal of Hydronautics*, Vol. 7, No. 4, 1973, pp. 137–144.

[3]Jeffrey, N. E., "Influence of Design Features on Underwater Towed System Stability," *Journal of Hydronautics*, Vol. 2, No. 4, 1968, pp. 205–212.

[4]DeLaurier, J. D., "A Stability Analysis of Cable-Body Systems Totally Immersed in a Fluid Stream," NASA CR-2021, April 1972.

[5]Abel, J. M., "Cable Interactions in a Depth Controlled Submersible," *Journal of Hydronautics*, Vol. 6, No. 2, 1972, pp. 83–89.

[6]Huffman, R. R., and Genin, J., "The Dynamical Behaviour of a Flexible Cable in a Uniform Flow Field," *Aeronautical Quarterly*, Vol. 22, May 1971, pp. 183–195.

[7]Cannon, T. C., and Genin, J., "Three-Dimensional Dynamical Behaviour of a Flexible Towed Cable," *Aeronautical Quarterly*, No. 23, Aug. 1972, pp. 201–210.

[8]Choo, Y., and Casarella, M. J., "Configuration of a Towline Attached to a Vehicle Moving in a Circular Path," *Journal of Hydronautics*, Vol. 6, No. 1, 1972, pp. 51–57.

[9]James, C. R., and Steven, A. C., "Dynamics of Cables Towed from Aircraft," USAF Academy Research Rept. 72-8, Oct. 1972.

[10]Russell, J. J., and Anderson, W. J., "Equilibrium and Stability of a Circularly Towed Cable Subject to Aerodynamic Drag," *Journal of Aircraft*, Vol. 14, No. 7, 1977, pp. 680–686.

[11]Calkins, D. E., "Hydrodynamic Analysis of a High-Speed Marine Towed System," *Journal of Hydronautics*, Vol. 13, No. 1, 1979, pp. 10–19.

[12]Sanders, J. V., "A Three-Dimensional Dynamic Analysis of a Towed System," *Ocean Engineering*, Vol. 9, No. 5, 1982, pp. 483–499.

[13]Delmer, T. N., and Stephens, T. C., "Numerical Simulation of Towed Cables," *Ocean Engineering*, Vol. 10, No. 2, 1983, pp. 119–132.

[14]Chapman, D. A., "The Adjustment of Fin Size to Minimise The Ship Induced Pitching Motion of a Towed Fish," *Ocean Engineering*, Vol. 11, No. 1, 1984, pp. 23–64.

[15]Chapman, D. A., "Towed Cable Behaviour During Ship Turning Manoeuvres," *Ocean Engineering*, Vol. 11, No. 4, 1984, pp. 327–361.

[16]Dreyer, T. P., "On The Modeling of Two-Dimensional Segmented Representations of Cable Shape," *Ocean Engineering*, Vol. 11, No. 6, 1984, pp. 609–625.

[17]Washizu, K., "Variational Methods in Elasticity & Plasticity," 3rd ed., Pergamon, Oxford, England, UK, 1982, pp. 556–567.

[18]Casarella, M. J., and Parsons, M., "Cable Systems under Hydrodynamic Loading," *Marine Technology Society Journal*, Vol. 4, No. 4, 1970, pp. 27–44.

[19]Hoerner, S. F., "Fluid Dynamic Drag," 1965, Chap. 3.

[20]Eames, M. C., "Steady-State Theory of Towing Cables," *Transactions of the Royal Institution of Naval Architects*, Vol. 2, No. 2, 1967, pp. 185–206.